# REMOVAL Of Fe $^{2+}$ and Fe $^{3+}$ FROM AQUEOUS SOLUTION USING RAW COWPEA HUSK, AND COWPEA HUSK COATED WITH ZINC OXIDE NANOPARTICLE ADSORBENT

**Khalaf Ahmed Abdullah* , Khalid Khazal Hummadi**

Department Environmental Engineering , college of Engineering , University of Baghdad , Iraq,
*Khalaf.abdallah2011m@coeng.uobaghdad.edu.iq

**Abstract**

In this study, cowpea husks were used as an adsorption media to recover Fe2+ and Fe3+ from aqueous solutions. Two of the media employed were raw cowpea husk (CPH) and cowpea husk coated with nano-ZnO. (CPHC). SEM, X-ray diffraction, and (FTIR) methods were utilized to evaluate the functional groups, morphological, structural, and percentages of surfactants (SEM),. To create the ideal situation, a number of factors counting pH, connection time, dose, beginning levels, and temperature were altered. The types of interactions involved were identified and described using thermodynamic simulations, adsorption isotherms, and thermodynamic studies. Under ideal conditions, the clearance rates of Fe2+ and Fe3+ varied from 76% and 70% to 94% and 920%, respectively. The removal efficiency rose somewhat with temperature, according to a thermodynamic study based on a optimistic sign of H°, proving the endothermic character of the adsorption process. When the data were fitted using the "Langmuir model", it was clear that the amount of adsorbent was homogeneous ($R^2$ values for CPH and CPHC, respectively, were 0.959 and 0.923 and 0.972 and 0.935 for $Fe^{2+}$ and $Fe^{3+}$). The "second-order kinetic model" providing the best explanation for the investigational consequences, which resulted in the conclusion that chemisorption was the main mechanism underlying the adsorption procedure.

**Keywords** Adsorption · Cowpea husk · ZnO nanoparticles · kinetic. heavy metals

## 1.      Introduction

pollution of heavy metals is a growing problem nowadays because of industrial development, agricultural activities, and transportation methods. The number of ions dumped as waste in the water body is increasing as industrial development picks up speed. Because of their well-known toxicity, heavy metals have been the subject of extensive research in the fields of water, wastewater, and effluent treatment. "Lead (Pb), chromium (Cr), cadmium (Cd), mercury (Hg), copper (Cu), nickel (Ni), ferris (Fe2+), and ferric (Fe3+) are some dangerous heavy metals found in the water body"[1]. Among the main heavy metal pollutants in water sources are Fe2+ and Fe3+. Due to their toxic effects on all living things, persistence in nature, and difficulty in being changed by microorganisms, heavy metals are difficult to properly dispose of into water bodies, even at low concentrations [2]. As a result, they build up in the ecosystem.

Significant concentrations of iron ions can happen due to a specific geological formation or contamination from industrial activities like the production of galvanized pipes, engine parts, and pipeline corrosion. Iron is one of the heavy metals with a high toxicity since it poses a digestive

risk when it builds up in the body (ll). Iron-loading and possibly neurological problems in certain tissues and cells, it might be precipitated of iron ions at high levels. under aerobic circumstances at a neutral or alkaline pH as an insoluble $Fe^{3+}$- hydroxide. Turbidity, an unpleasant taste and odor, and vomiting can all be caused by an excessive level of Fe(ll) and Fe(lll) in public water supplies [4].

Adsorption is a process used to treat wastewater to get rid of contaminants such heavy metals, pigments, and antibiotics. The two main categories of adsorption techniques are chemisorption and physisorption. Sorption process is reversible because there are relatively weak forces between both the adsorbed species and internal cohesion. Chemical adsorptions, on the other hand, result in strong forces developing between the adsorbed species and the hard surfaces. Chemical adsorption experiments may make it difficult to identify adsorbates from solid surfaces. Adsorption is superior to other processes in a number of ways that make it ideal for treating water, including the potential for product recovery and the capacity of solutions for fully automated, unsupervised procedures for completely automated, unsupervised operating, superior control, and response to process modification [5].

Nano generators are just one application for which ZnO nanoparticles are potential prospects. The "high surface-to-volume ratio" of nanoparticles is one of their distinctive characteristics, which adds to their allure. Because atoms on the surface tend to be more active than those in the middle, this property of nanoparticles makes them more reactive than the bulk material. The processes used to create these nanoparticles can be physical, chemical, or biological. Different physical and chemical processes including hydrothermal, sol-gel synthesis, laser ablation, and lithography, among others, call for specialized tools and trained personnel. They also have harmful effects. The green synthesis approach produces nanoparticles that are determined to be naturally non-toxic, biodegradable, and cost-effective [6].

Heavy metal waste can be reduced in a several methods counting adsorption, ion exchange, flotation, and filtration. Adsorption is a suitable approach among these due to its straightforward operation, low cost, and quick process. Many different adsorbents, including cellulose and layered double hydroxides, have been utilized for metal ion adsorption [7]. Zeolite [8]. Bentonite [9]. Cowpea husk (CPH) coated with ZnO was used in this study. One of the most significant tropical dual-purpose legumes is the cowpea. It is used for hay and silage cowpea husk (CPH), fresh cut-and-carry greenery, grain, leafy vegetables, and hay. Cowpea husks were gathered from fields in the surrounding area; they are brown in color, light in weight, and crispy. With the aid of an electric mill, the husks were ground. This report's species under study is one that is found in the area[10]. Due to their significantly reduced cost, cowpea husk and cowpea husk coated /ZnO (CPHC) wastes were examined in this study to remove irons metals from wastewater.

## 2.    "MATERIALS AND METHODS"
### 2.1 "Materials"

Ferric has the "chemical formula Fe (No3)3.9H2O" and has a molecular weight of 404.00 whereas Ferris has the formula Fe (No3)2.6H2O and has a molecular weight of 179.86. were purchased

from an Indian central drug house; Adding "0.1 mol/L of sodium hydroxide or hydrochloric acid (HCl)" kept the pH constant throughout the experiment (NaOH). The nanoparticles of 99% pure zinc oxide (ZnO), 30–40 nm in size. Without additional purification, acetonitrile from Sigma-Aldrich (Milan, Italy) was used.

### 2.2 Adsorbent preparation

The cowpea husk coated (CPHC) adsorbent for the current experiment was made using the basic method below. Cowpea peel was picked locally, cleaned by hand, thoroughly rinsed with distilled water, soaked for a few hours, and then dried for twenty-four hours at 105 °C in an appropriate oven. The treated dry peels had been crushed and sieved to a specific particle size of 125 m. Small samples of the generated (CPH) were taken for analysis, and ZnO nanoparticles were applied to the surfaces of the remaining samples. A appropriate dispersion (acetone) was combined with ZnO nanoparticles obtained from manufactured ZnO nanoparticles. The cowpea husk coated (CPHC) adsorbent for the current experiment was made using the basic method below. Cowpea peel was picked locally, cleaned by hand, thoroughly rinsed with distilled water, soaked for a few hours, and then dried for twenty-four hours at 105 °C in an appropriate oven. The treated dry peels had been crushed and sieved to a specific particle size of 125 m. Small samples of the generated (CPH) were taken for analysis, and ZnO nanoparticles were applied to the surfaces of the remaining samples. A appropriate dispersion (acetone) was combined with ZnO nanoparticles obtained from manufactured ZnO nanoparticles, and the combination was then stimulated in a magnetic stirrer for 30 minutes.

**Fig (1) : The cowpea husk collection(a), The cowpea husk ground(b), ZnO nanoparticles(c), The cowpea husk after coating with ZnO nanoparticles(d)**

### 2.3 Characterization of CPHC

The following analyses were used to look into the characteristics of the adsorbent: With a 10-KV potential and a 6-mA fluorescence, a SEM (NOVASEM, FEL450L) was used to analyze the adsorbent's surface properties. This experiment demonstrates how the adsorbent's structural properties change both before and after the $Fe^{2+}$ and $Fe^{3+}$ are removed. The experiment was conducted at the University of Tehran's College of Science. SEM and chemical microanalysis are combined in the process. It is used to determine the atomic make-up of a material. This examination was held at the University of Tehran's College of Science. In order to discover functional groups on surfaces, researchers have devised a method called "Fourier transform infrared spectroscopy" (FTIR). This work presents a method for spectrophotometric monitoring. A "Bruker Tensor 27 spectrophotometer and the KBr pellet" method was utilized to investigate the spectra in the 40 hundred to 40 thousand cm-1 range. You can obtain it at the University of Tehran's College of Science.

### 2.4 Adsorption experiments

In this research, batch test is used to determine the optimum conditions for raw cowpea husk. Different parameters were studied such as concentration, contact time, initial concentration, and pH. Each experiment involved shaking an orbital shaker for a predetermined amount of time with a 250 ml flask containing 100 ml of fluid. The sample was subsequently filtered, and the concentration of heavy metals was determined using an "atomic absorption spectrophotometer." The following formulae were used to obtain the optimum sorption (qe, mg/g) and the removal efficacy (%), respectively. (1,2) [12].

$$qe = \frac{(co-c\ )v}{w} \qquad\qquad (1)$$

$$R\% = \frac{Co-C}{Co} \times 100 \qquad\qquad (2)$$

"Where V is the sample volume (in L), Co and Ce are the heavy metal's starting and optimum levels (in mg.L$^{-1}$ and mg. L$^{-1}$ , respectively), and W is the amount of the adsorbed that was used (g)."

### 3.     Adsorption Equilibrium Models

### 3.1 Thermodynamic study

It is possible to establish whether a reaction is spontaneous by looking at how temperature affects the "adsorption process". It is possible to evaluate the propensity for spontaneity of the adsorption reaction using thermodynamic metrics. Each of these parameters was computed using the formulae listed below. (3,4) [13].

$$\Delta G^0 = -RT \ln K_C \qquad\qquad (3)$$

$$\Delta G^0 = \Delta H^0 - T\Delta S^0 \qquad\qquad (4)$$

"where R is the universal gas constant (8.314 J/mol.K), T is the absolute temperature (K) and Kc is the distribution coefficient equals to qe/Ce. The values of ΔH and ΔS were calculated from the slope and intercept of the plot of ln Kc versus 1/T values of ΔG indicates that the process is feasible and the adsorption is thermodynamically spontaneous".

### 3.2    isotherm model

The equilibrium isotherm, which has been successfully described by multiple adsorption studies, is one of the crucial components that provides correct data for the study of the contaminants that are absorbed on different adsorbents. "The Langmuir and Freundlich" isotherms" were used as adsorption models to suit the experimental isotherm data provided in this investigation. Two popular isotherms for explaining equilibrium are the "Freundlich isotherm and the Langmuir adsorption" isotherm. The Langmuir model isotherm has an expression in each of the following expression (5 and 6).

"qe = qmax. KLCf/(1+KLCe)"                     (5)

" qe = kf $c e^{1/n}$          "                     (6)

"$q_{max}$: maximum adsorption capacity at complete monolayer coverage (mg/g); $q$e: equilibrium adsorbate uptake (mg/g); $C$e: equilibrium (final) concentrations of the sorbate (mg/L);$KL$ is defined as the affinity parameter related to the bonding energy of the sorbate; $kf$: Freundlich isotherm constant (mg/g).n: adsorption intensity" [15].

### 3.3    Kinetic Study

Giving the reaction route and the ideal absorption mechanism considerable importance necessitates the examination of kinetic models. In additional to the charge transport procedure, the sorption process also relies on its biological and chemical properties [15]. One of the most crucial factors affecting how effective adsorption is is the adsorption kinetics. One step—or any mixture of them—can act as the percentage mechanism: Adsorption (physical or chemical), which is typically thought to happen very quickly, at a place on the membrane (internal or exterior), as well as mass transfer through the liquid film that creates the particle's outer boundary layer, and iii. migration of the adsorbed molecules to the adsorption site through either a hole Diffusion process. The third model serves as the foundation for diffusion rate limiting analysis. The "pseudo-first order Lagrange model" can be described using the following equations in light of this.

" $\frac{dqt}{dt}$= K (qe - qt)"                     (7)

"The integral form of this equation is given as follows":

"ln (qe - qt) = ln qe- k1t"                     (8)

"Where qe is the equilibrium adsorption capacity of the adsorbent (mg / g), qt is the adsorption capacity (mg / g) when the contact time is t, K and k1 are the rate constants of the pseudo first-order adsorption model."

"The adsorption kinetic may be described by the pseudo-second-order model. The linear equation is generally given as follows equation respectively (9)(10)":

"$\frac{dqt}{dt} = k_2(qe - qt)^2$"                    (9)

"The integral form of this equation is given as follows":

"$\frac{t}{qt} = \frac{1}{k2qe2} + \frac{1}{qe}t$"                    (10)

"where qe is the equilibrium adsorption capacity of the adsorbent (mg /g), qt is the adsorption capacity (mg / g) when the contact time is t, k2 is the rate constant of the pseudo second-order adsorption model."

"The Intraparticle diffusion model can be expressed as follows equation (11)":

"$q_t = k_d t^{\frac{1}{2}} + C$"                    (11)

"Where qt (mg / g) is the adsorption capacity at time t (min), kd (mg / g.min–0.5) is the intraparticle diffusion rate constant, and C (mg / g) is the intercept which represents the boundary layer thickness."

## 3.4     "Determination of pH of point zero charge (pHpzc)"

The "pHpzc" of CPH and CPH/ZnO was calculated using a detailed methodology [17]. As a result, the preliminary pH standards were altered from 3 to 11, and a 100 mL solution containing 50 mg/L was poured into 16 beakers. The exact amount of 0.5 g of "0.1 M NaOH or HCl" concentrations, dried powdered CPH, or CPH/ZnO, was added to flask and mixed for 24 hours. The pHpzc could be calculated since the starting and final pH curves intersected.

## 4.     Results

### 4.1 "Characterizations of Adsorbents"

### 4.1.1 "FTIR Analysis" (CPH  and CPH/ZnO  )

An analytical test method called "FTIR spectroscopy" is used to distinguish between chemical, polymeric, and sometimes mineral substances. FTIR technology scans test materials and keeps track of chemical characteristics using infrared light. Infrared light from the analysis tool is emitted, and the sample particles absorb this light and convert it into rotating or vibrating energy. Figure (3) shows the primary functional groups that boosted the elimination of heavy metals from the non-modified adsorptive using FTIR spectra collected in the region of 4000 cm-1 to 450 cm-1 both before and after sorption (cowpea husk).

Observed at 3672.8 cm1, this high-intensity absorption band is the result of bending vibration of hydroxyl groups (O-H) in the high wavenumber range [18]. Additionally, the stretching vibrations between 3294.15 and 3340 cm-1 are activated (C-H). A weaker band caused by the bending of H-O-H has been seen at 1664.52- 1417.83 cm-1 [19]. The currently available cowpea husk samples exhibit C=O stretching due to doubly degenerate asymmetric stretching vibration at wavenumbers of 1361.24 cm-1 and also at 782- 693.55 cm-1 [20]. The Si-O-Si bond developed in a discrete adsorption region between 1091.61 and 1098.84 cm1. The O-Si-O vibrations at 580.94 cm1 establish the presence of quartz, although this quartz is believed to be crystalline because of the band at 418.60 cm1. The intensity of the acute adsorption band and the extent of their vibration after adsorption change. Wavenumbers between 3700 and 3500, 2800 and 2700, 1000 and 1100, and 700 and 600 cm-1 were discovered to display a displacement in intensity, indicating that the active groups that are present at these wavelengths are what cause the adsorption process [21].

Figure 1 displays the coated adsorbent's FTIR spectra both prior to and after adsorption (4). [129] asserts that the peak between 890 and 1082 cm-1 is regarded as a region that can be utilized to identify carbohydrates. The activation of the C-N group is what generates the bending vibration at 916 cm1. The C-H group received maxima at 1300 and 1385 cm-1 with roughly equal intensity. The carboxyl group and C=O are responsible for the absorption of 1620 and 1640 cm-1. The weak band at 2849 cm-1 is associated to C=O bonds from carbonate, while the broad transmitting group at roughly 2894 cm-1 is created by C-O stretching vibration caused by the presence of carbonate [22]. The extending shaking of the O-H groups is what generates the 3692 cm-1 observed peak. Additionally, each and every peak at 1590 cm1 is linked to the extending and bending vibration of N-H groups [23]. According to the FTIR spectra, the raw and chemically changed Cowpea husk is discovered to include a variety of functional groups. According to the findings, bands with hydroxyl and carbonyl groups migrated to reduced dispersion and are therefore essential to the adsorption process.
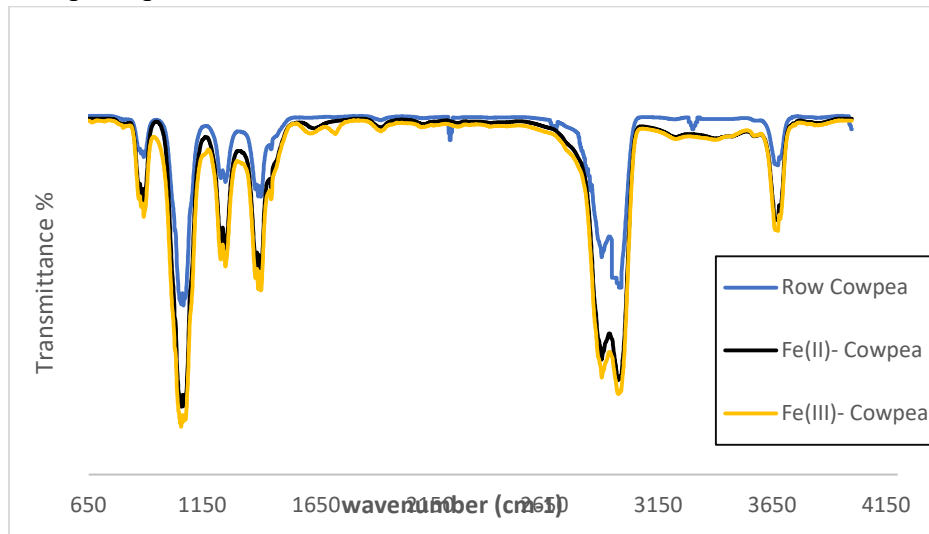


Fig. 3: 1 FTIR Analysis spectrums for row cowpea husk before and after sorption of metal ions
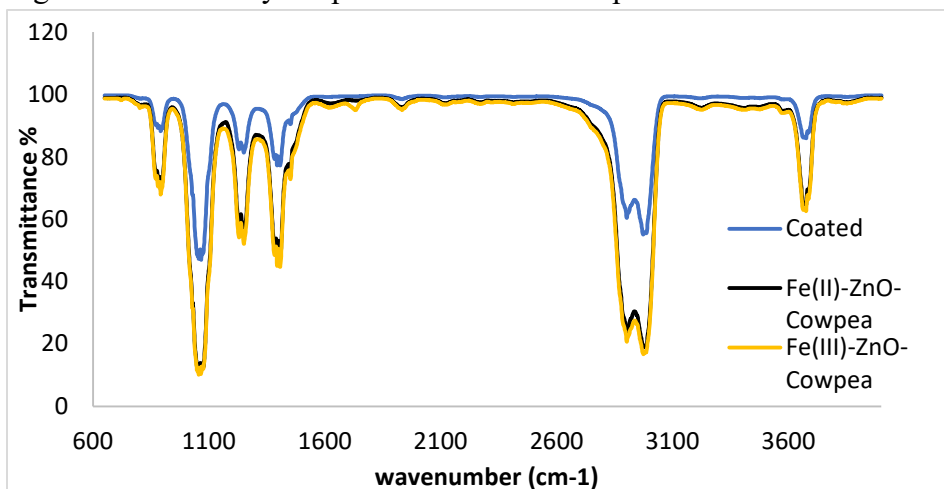


Fig. 4: FTIR Analysis spectrums for coated cowpea husk before and after sorption of metal ions.

### 4.1.2 The X-ray Diffraction (CPH and CPH/ZnO )

Figure shows the X-Ray diffraction pattern of row cowpea husk both before and after adsorption (5). 37 diffraction peaks can be seen in the diffraction pattern. 16.9, 18.9, 25.15, 29, 32.1, 36.2, 41.2, 50.4, 52, 56.5, and 62 were the major peaks. Zirconia and Potassium Aqua Molybdenum Oxide, Zinc Oxide, and Vanadium Zirconium Fluoride, which have the chemical formulas $Zr O_2$, $K_{0.23} (H_2O)_{0.27} Mo O_3$, and $V Zr F_6$, respectively, make up the majority of the composition. According to the "Joint Committee on Powder Diffraction Standards (JCPDS)", these compounds' references codes are 00-013-0307, 00-052-0178, 01-075-0576, and 01-081-1939. The results of the row adsorbent and metals-adsorbent (i.e., post adsorption) XRD examinations do not clearly differ from one another. This suggests that physical adsorption is the mechanical control of the removal process and that there has been no change in the chemical makeup of the adsorbent. The coated cowpea husk's XRD patterns are shown in Figure (6) both before and after adsorption. The diffraction peaks of the native, chemically modified, and adsorbate-adsorbent patterns of analysis are comparable. There are 14 diffraction peaks visible in the diffraction pattern. The principal peaks occurred at (2) 16.1, 22, 24.2, 32, 33.8, 48, 65.9, and 75. The raw sample, which contains the phases quartz and cristobalite, was represented by the largest adsorbent peaks between 21° and 47.5°. All XRD analysis tests showed that there have been no significant changes to the composition and structural characteristics overall. Thus, it can be said that the removal of heavy metals is only surface treatment [24].
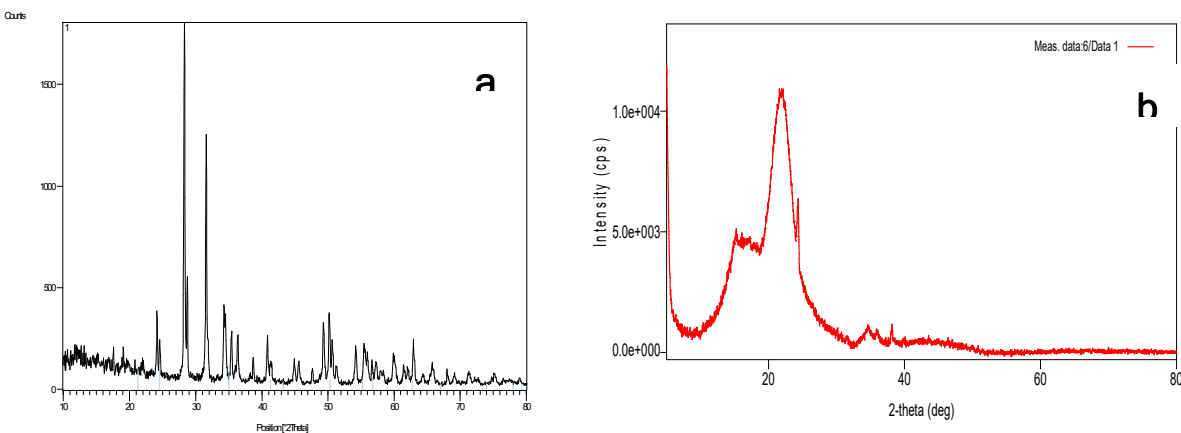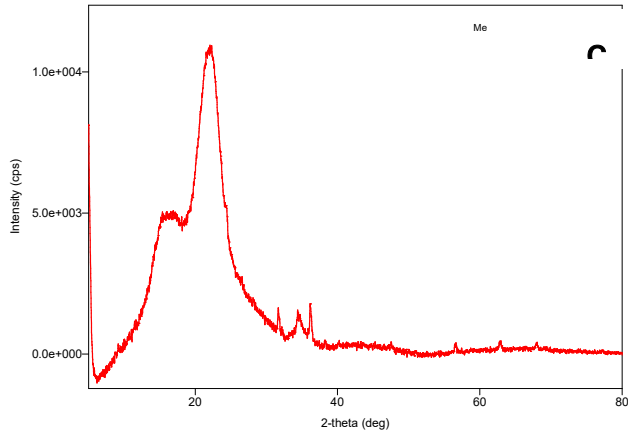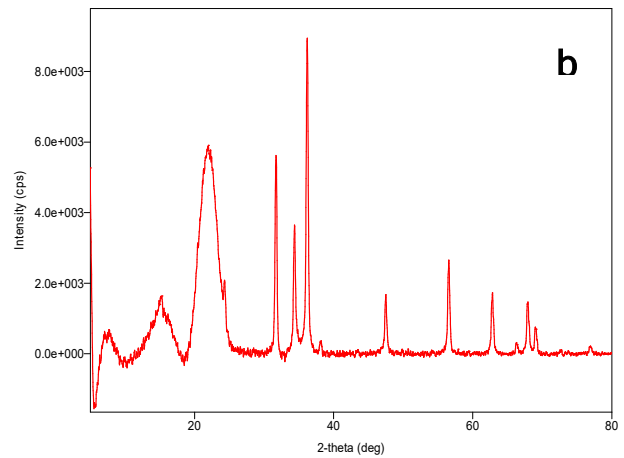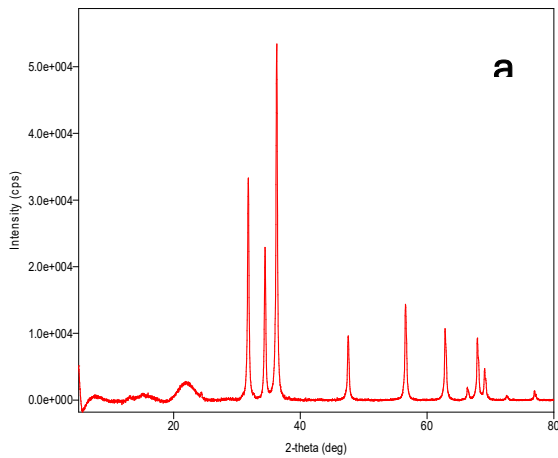
Fig. (5): The "XRD pattern" of row cowpea husk before and after sorption of metal ions: a) row Cowpea husk adsorbent, b) Fe (II)- Cowpea husk adsorbent, c) Fe (III)- Cowpea husk adsorbent.
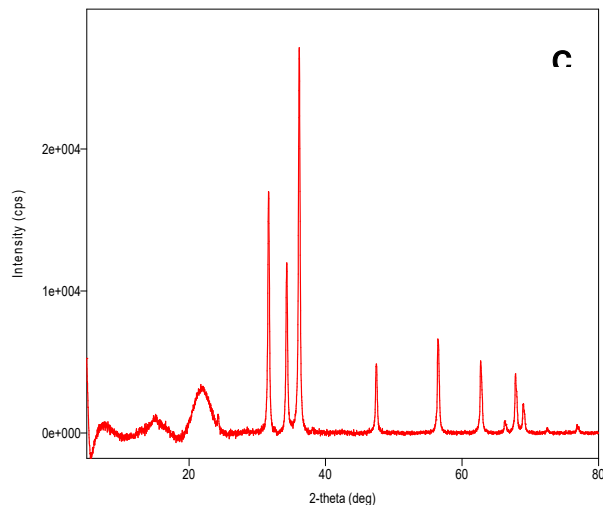
Fig.(6) : The "XRD pattern" of row cowpea husk before and after sorption of metal ions: a) coated Cowpea husk adsorbent, b) Fe (II)- Cowpea husk adsorbent, c) Fe (III)- Cowpea husk adsorbent.

### 4.1.3 Scanning Electron Microscope (CPH and CPH/ZnO)

SEM analysis of row cowpea husk before and after adsorption reveals a wide range of irregular sizes and shapes of grains, as shown in figure. This analysis is done to learn more about the surface morphology, microstructures, and crystalline phases of row and chemically coated cowpea husk before and after adsorption (7). There are many different sizes and shapes of intragranular pores. These adsorbents' comparatively high porosity is caused by a combination of uneven particle size and shape and high intragranular porosity, which denotes significant surface areas. After adsorption, the surface's shape is more regular and homogenous. compared to cowpea husk, which could be attributed to the contaminants that filled these holes and grooves.

Figure (8) shows the SEM images that showed the coated adsorbent's direct internal structure both before and after treatment. The coated adsorbent also exhibited porous morphology, indicating a greater specific surface area, in addition to the microspore structure. The morphology of the surface after adsorption differs from row adsorbent and is irregular; this could be because of contaminants that scatter the surface.
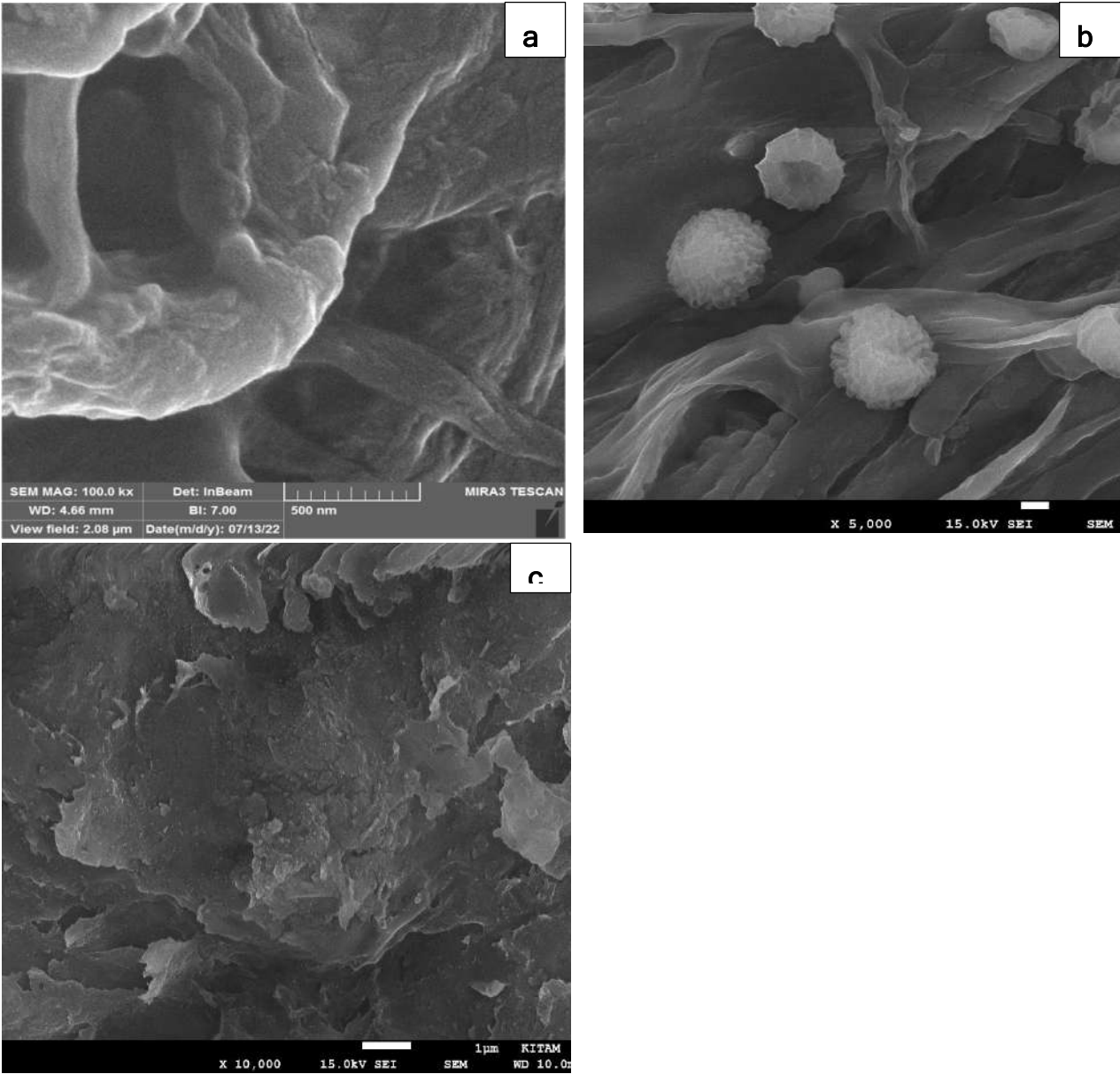
Fig.(7) : The SEM pattern of row cowpea husk before and after sorption of metal ions: a) row Cowpea husk adsorbent,  b) Fe (II)- Cowpea husk adsorbent,  e) Fe (III)- Cowpea husk adsorbent.
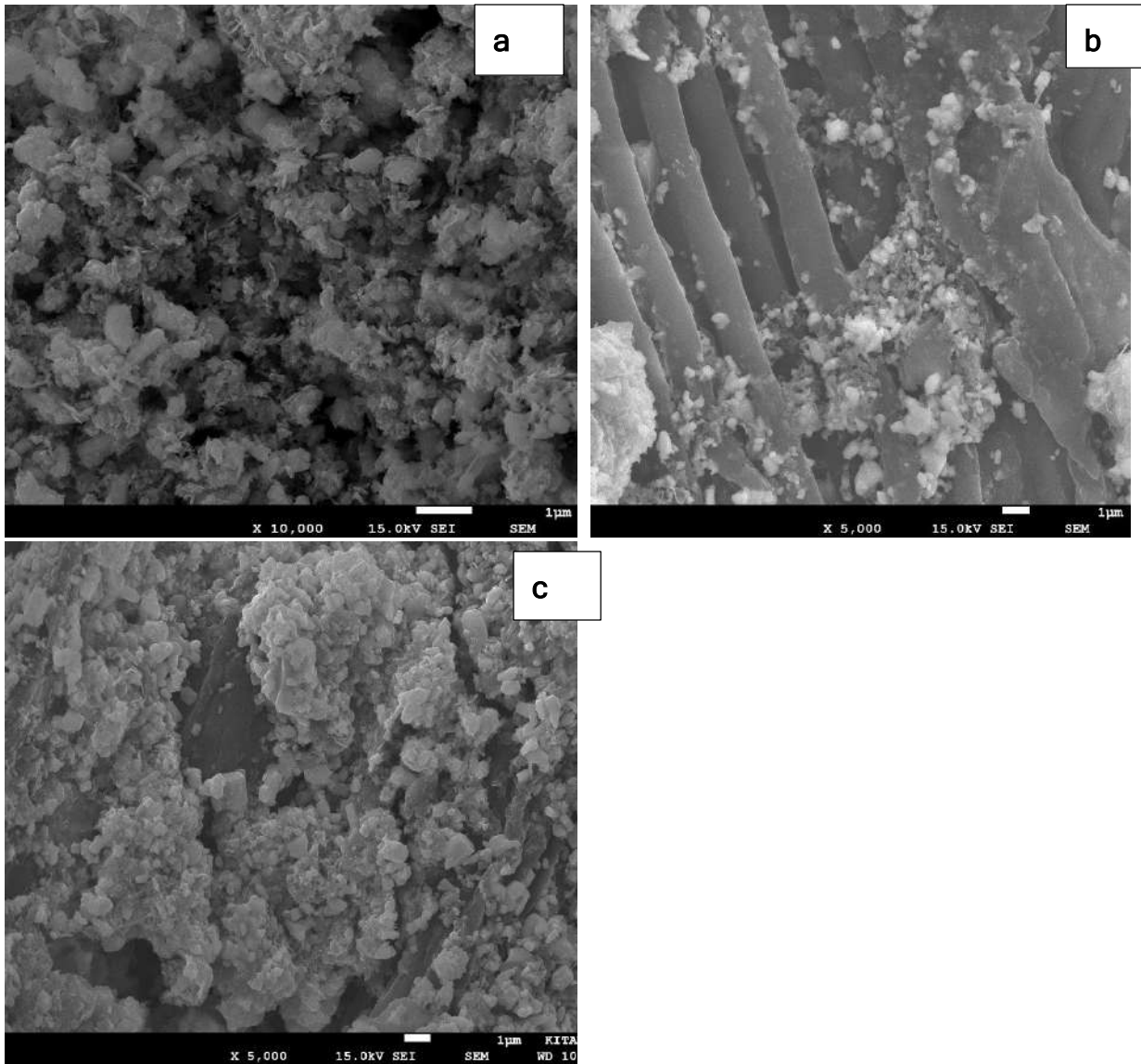
Fig. (8) : The SEM pattern of coated cowpea husk before and after sorption of metal ions: a) coated Cowpea husk adsorbent,  b) Fe (II)- Cowpea husk adsorbent,  c) Fe (III)- Cowpea husk adsorbent.

**4.2 Effects of Experimental Parameter.**

**4.2.1 "Effect of Dosage on Removal Efficiency"**

Because adsorbent dose determines an adsorbent's capacity several effects for the adsorbent are investigated. The relation between the amount of adsorbent and the elimination efficiency is opposite [25]. The influence of the dosage on the removal % at different tested doses that ranged from 0.1 to 2 g/100 ml was explored in order to attain the best removal efficiency. It is evident in which the removal capacity increased with increasing mass transfer for the adsorbent, as shown in Figure 9. Two types of iron metals removal effectiveness on the surface of the cowpea husk increases from (44% and 37%) to (66% and 59%), respectively. However, the removal rates on

coated adsorbent for two types of iron metals, respectively, rose from (53% and 49%) to (74% and 79%). It is also claimed that coated adsorbent has a higher efficiency to remove metal ions from effluent as the chemical and physical properties of adsorbent media are enhanced through adsorbent modification.

Numerous studies have shown that as the quantity of the surface-assimilative is raised, an increased percentage of the metal ions are removed [26]. Due to an increase in adsorbent mass, these properties were thought to be caused by a greater availability of adsorption sites. Similar results were found by [27]. On the other hand, it is found that as adsorbent doses are raised, the adsorbent's maximal adsorption capacities decline. According to figure 10, the removal percentage of Fe (III) fell from 68% to 59% and (88% to 79%) as the mass increased from 0.5 to 2 g of row and coated adsorbent, respectively. Additionally, the removal percent drops from (73% to 66%) and (85% to 74%) as the mass rises from 1 to 2 g of row and coated adsorbent. The impact of overlapped adsorption active sites, which decreased both the overall attached surface area of the material and the amount of energetic locations that were available, was blamed for the decline in removal efficacy
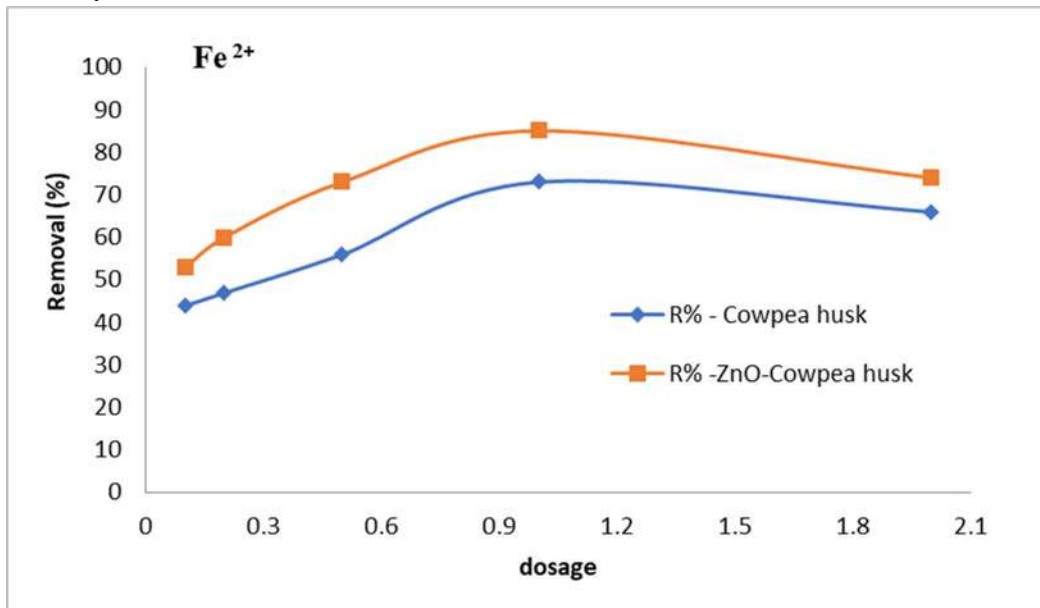


[28].
Fig. (9): "Effect of dosage on the Adsorption of Fe (II)" onto row and modified cowpea husk, (pH=5, Co=50 mg/l, time=120min, particle size =125μm, and 150 rpm).

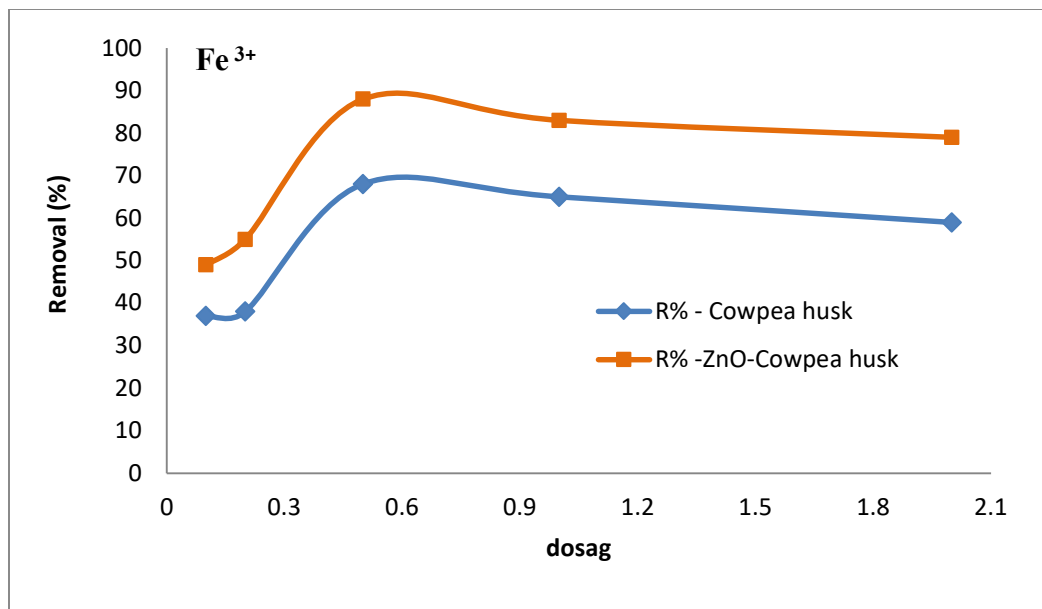Fig. (10): "Effect of dosage on the Adsorption of Fe (III)" onto row and modified cowpea husk, (pH=5, Co=50 mg/l, time=120min, particle size =125µm, and 150 rpm)

## 4.2.2 Effect of Initial concentration on Removal Efficiency

The force between the two types of materials can overcome the resistance of the solution in which controls the charge transfer of solute molecules between the solid and aqueous phases. As the beginning level of the pollutants of the two types of iron metals, the efficiency of the elimination decreased, according to the study's findings. In accordance with Figure (11), (12). The processes were performed at different initial concentrations of two types of iron metals ranged from ten to one hundred in mg/L. The elimination effectiveness of Fe (II) and Fe (III) also drop from 53% and 43% to 73% and 70%, respectively, on the row adsorbent. On the coated cowpea husk figure, elimination of Fe (II) and increased from 73% to 82% for the both Fe (II) and Fe (III). A higher concentration implies the presence of more metal ions. One reason as to why mass transfer increases as metal ion concentration in solution rises is increased in which the transport of ions to the surface is occurred. After crossing this threshold, the clearance % starts to decline as the original concentration of heavy metals increases. This is because the adsorbent sample lacks sufficient binding sites to allow for the metal ion adsorption. The effect of the initial concentration was explained as down below: When the ratio of adsorbent to contaminant is low, there are more energy-binding sites involved in contaminant adsorption. As the ratio of heavy metals to adsorbent increases and the increasing and the decreasing related to the binding energy between molecules [21]. The fact that the adsorbate uptake (qe) increases as the beginning concentration increases during the course of the detention time is also noted. The initial mass of heavy metals in solution establishes the qe values; high initial concentrations cause an increase in metal mass that easily

transfer                           to                           an                           adsorbent                           surface.
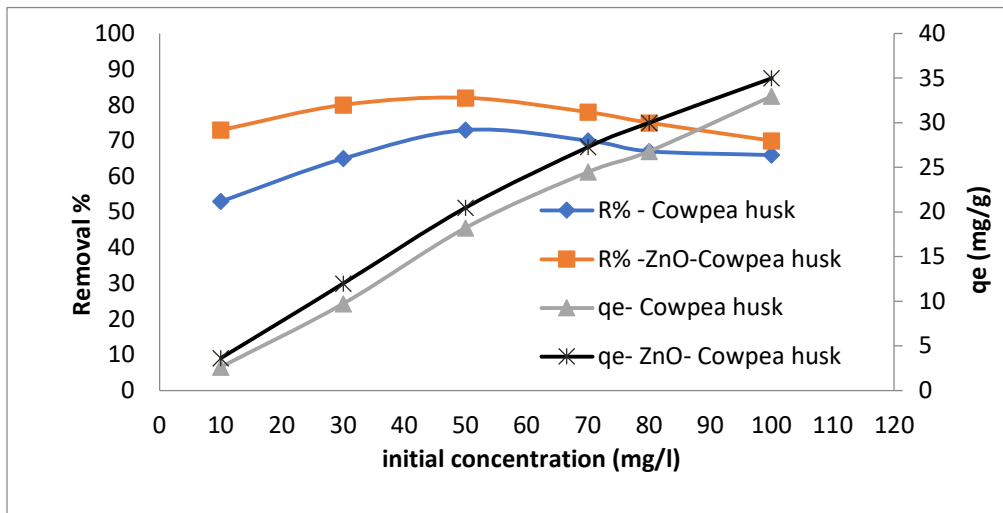


Fig. (11): "Effect of concentration on the Adsorption of Fe (II)" onto row and modified cowpea husk, (pH=5, dose=1 g/100 ml, time=120min, particle size =125μm, and 150 rpm)".
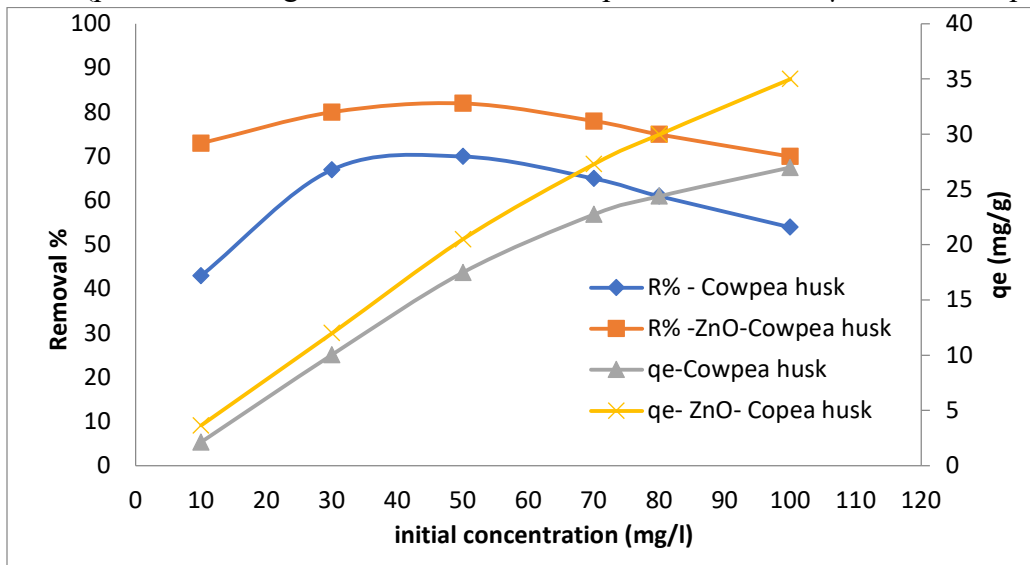


Fig.(12): "Effect of concentration on the Adsorption of Fe (III)" onto row and modified cowpea husk, (pH=5, dose= 1 g/100 ml, time = 120min, particle size =125μm, and 150 rpm)".

### 4.2.3 "Effect of pH on Removal Efficiency"

To achieve the highest elimination ratio, solutions at various pH levels ranging from 3 to 11 were tested for the impact of pH. Due to repulsive forces, cations like (Fe 2+) adsorb best at pH levels above pHpzc, while anions prefer pH levels below pHpzc [29]. The examination of pHpzc Figure (13), which shows the pH level is being neutrally charged at the surface of materials, is crucial in this direction. The pHpzc of the Cowpea husk and Cowpea husk coated were found to be 6.1 and 7, respectively, after analysis. It's also vital to remember that ZnO nanoparticle surfaces often contain neutral-charged hydroxyl (OH) groups. Depending on the pH level, this group's charge may change [30]. The H+ ions leave the adsorbent layer at pH > pHpzc because ZnO has a negative

charge. At pH pHpzc, H+ ions migrate to the adsorbent surface and linked with OH- groups, resulting in the creation of ZnOH2 + groups [11].

Figures (14) & (15) make it quite evident that as pH increased, metal ion removal efficiency improved (15). Thus, there may be an electrostatic attraction between them, leading to a high efficiency of metal removal. The decrease in adsorption effectiveness at pH 3 was caused by "electrostatic repulsion" between positively charged ZnO nanoparticles and "cationic heavy metal moieties". the percentage of removal with row and modified adsorbent when the pH is increased from 3 to 4. The results for "Fe (II) and Fe (III)" adsorption onto rows and modified adsorbents were the same; Fe (II) removal percentage increased from 39% and 67 to 46% and 72. Additionally, for row and modified adsorbent, the elimination ratios of iron metals rise from (28% and 57%) to (68% and 90%), respectively. The high elimination efficacy when the pH value is or above (5) the copper started precipitating as (Fe (OH)) could be attributed to the deposition of these metals and not as a result of the adsorbent efficacy, since it was noticed that heavy metals agglomerate and precipitate in alkaline solutions. Accordingly, it was decided that a pH of 4 was ideal
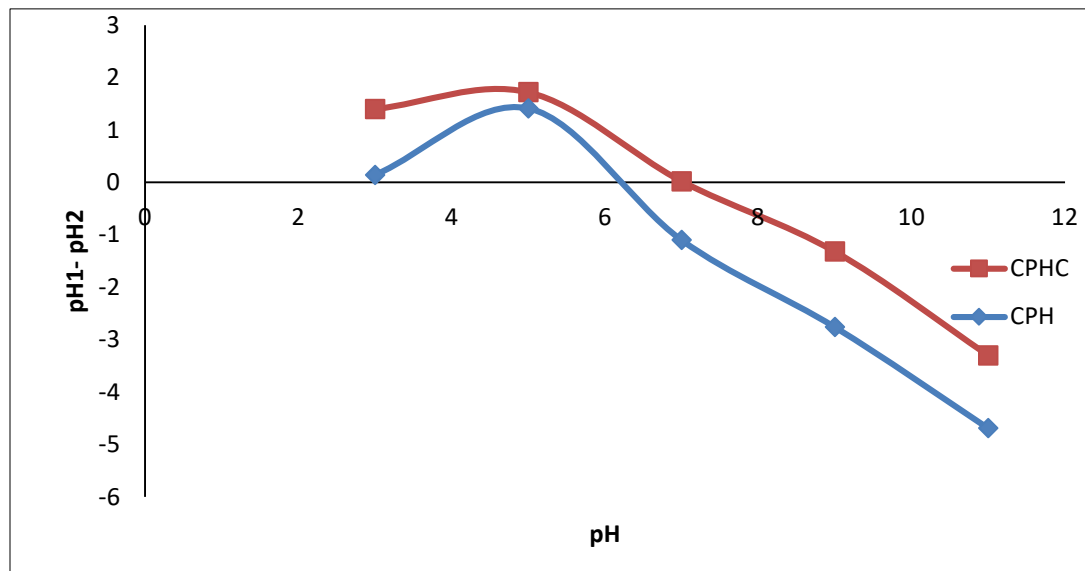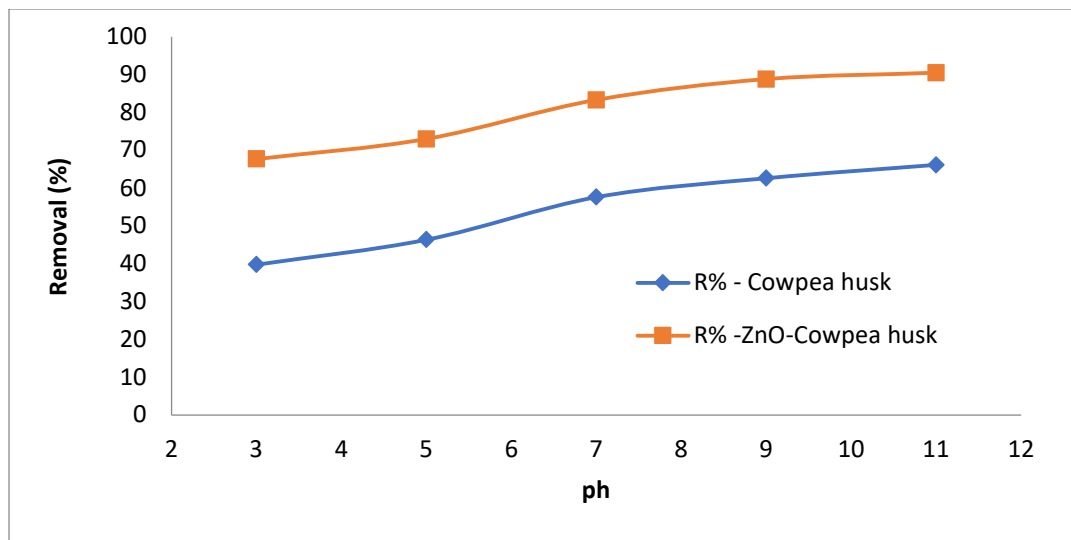


Fig. (13): pHpzc of Adsorbent

Fig.(14) : "Effect of PH on the Adsorption" of Fe (II) CPH  and CPH/ZnO  , (dose= 1g/ 100 ml, Co=50 mg/l, time=120min, particle size =125μm, and 150 rpm)
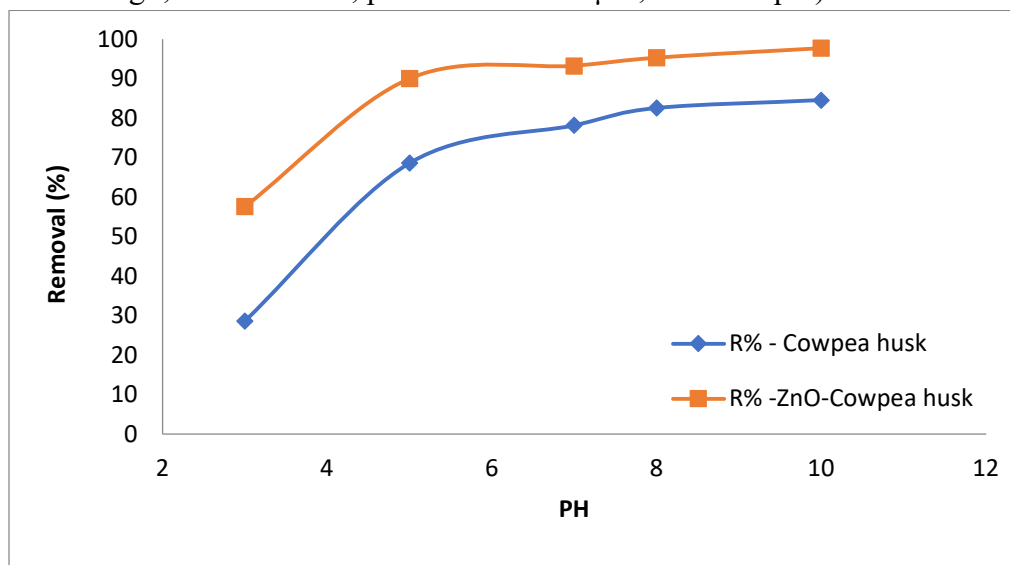


Fig.(15) : "Effect of PH on the Adsorption" of Fe (III) CPH  and CPH/ZnO  , (dose= 1 g/ 100ml, Co=50 mg/l, time=120min, particle size =125μm, and 150 rpm)

**4.2.4 "Effect of Detention time on Removal Efficiency"**

It is possible to estimate the required adsorption "equilibrium time" on metal ion elimination was investigated. When the adsorbent's surface was not covered in metal ions, it was found that adsorption occurred quickly. It should be noted that for the row and coated adsorbent, the removal percentage of Fe (II) rose as the retention duration increased, reaching 76.58% and 91.82 after 210 min., respectively. On the row surface of cowpea husk, the percent removal for the Fe (III) was 20.72% and 79.48% for 10 and 210 min, respectively, while the removal percent was 46.97 and 92.06% for the same period on the coated adsorbent.

The time was utilized in these experiments as 120 min. It becomes out that none of the initial concentrations significantly changed after these times. As a result, the adsorption rate started out

quickly before gradually slowing down due to saturation. The fast-phase sorption can be explained by bio-sorbent surface ion exchange or passive uptake via physical adsorption. Due to the immediate equilibrium that the adsorption phenomenon frequently achieves and the fact that A large number of farming wastes act as "natural ion exchangers". [31]. The uptake of metal by might begin immediately before active number of sites in which started to decease and these sites are located on the surface of the iron metal. This is because each active sorption site in a system can only adsorb one ion in a monolayer [32].
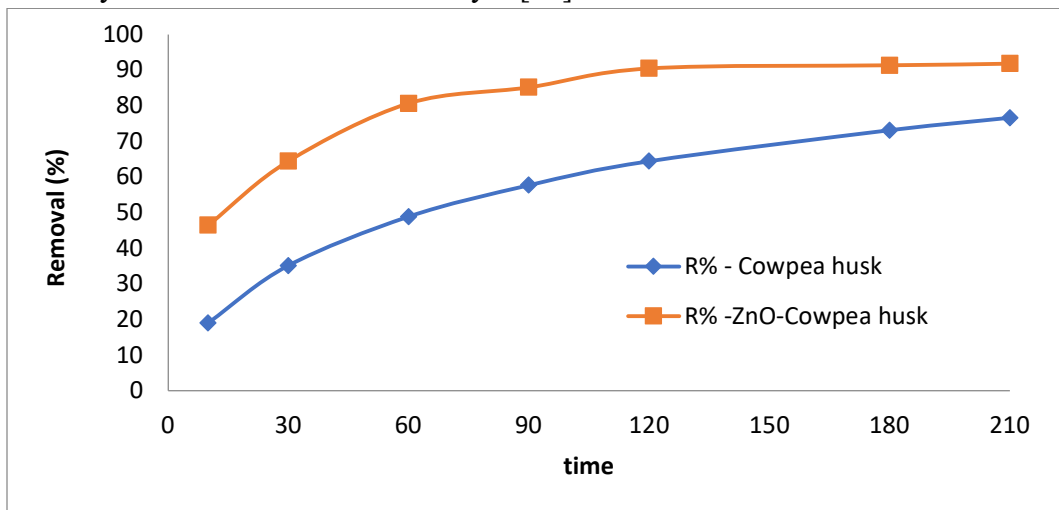


Fig. (16) : "Effect of Detention time on the Adsorption of Fe (II) CPH and CPH/ZnO , (dose= 1 g/ 100ml, Co=50 mg/l, pH=4, particle size =125µm, and 150 rpm)".



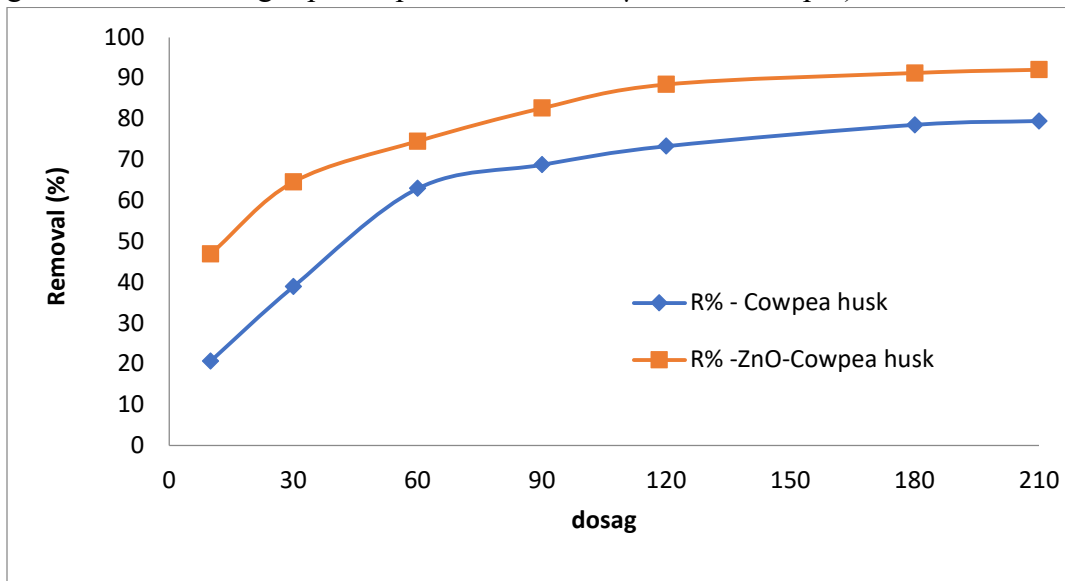Fig.(17) : "Effect of Detention time on the Adsorption of Fe (III CPH and CPH/ZnO , (dose= 1 g/ 100ml, Co=50 mg/l, pH= 4, particle size =125µm, and 150 rpm)".

### 4.2.5 "Effect of Temperature on the Removal Efficiency"

By adjusting the temperature, the temperature effect on the capacity of two types of metals ions was investigated. The data was analyzed, the tests were occurred at room temperature and that temperature differences between the research were often only a few degrees Celsius [33]. Due to the increased rate of adsorbed molecule diffusion via the interior pores and external boundary layer of the adsorbent particles caused by the higher temperature. Figures (18) and (19) show how different temperatures (15, 25, 35, and 45 C°) affect things. On the unaltered cowpea husk, it is seen that the elimination ratios of Fe (II) and Fe (III) rise from (69% and 61%) to (83% and 84%), respectively. On the improved adsorbent, however, the elimination rates of Fe (II) and Fe (III) rose from (76% and 70%) to (94% and 92%), respectively. This discovery demonstrated that the effectiveness of metal removal is enhanced as the temperature increased, indicating that the metals removal process is endothermic [34]. The number of molecules that can engage the surface's active site multiplies when there is enough energy (high temperature) present [35]. The internal-diffusion controlled adsorption mechanism increases the adsorption capability at high temperatures [36].
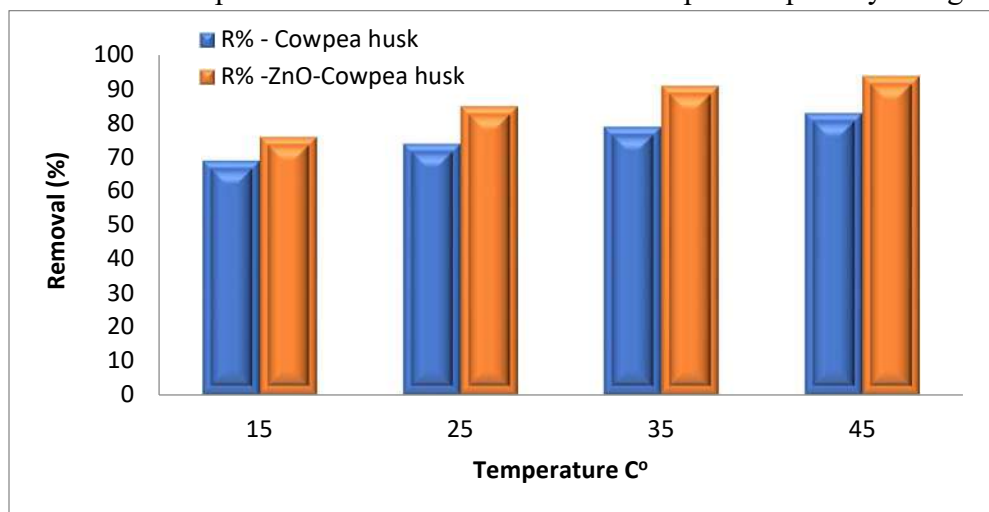


Fig. (18): "Consequence of Temperature on the Adsorption of Fe (II) CPH and CPH/ZnO , (pH=4, Co=50 mg/l, time= 120min, particle size =125µm, dose = 1 g/ 100ml, and 150 rpm)"
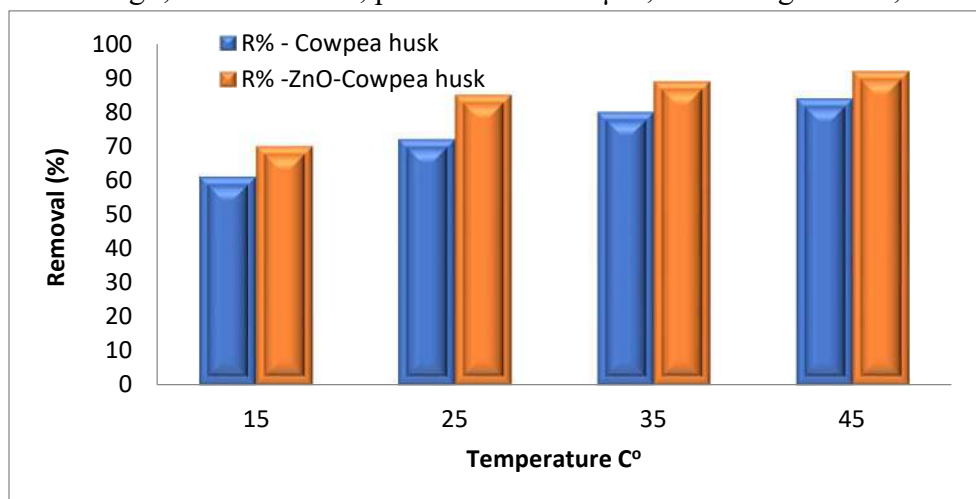
Fig. (19): "Consequence of Temperature on the Adsorption of Fe (III) CPH and CPH/ZnO, (pH=4, Co=50 mg/l, time= 120min, particle size =125µm, dose = 1 g/ 100ml, and 150 rpm)"

## 4.3. Thermodynamic Study

The results of analyzing the elimination effectiveness of two types of metals as a variation in temperature from twenty-five °C to forty-five °C are displayed in the following figures (20) (21). Thermodynamic adsorption of two types of metals onto coated and uncoated cowpea husk at various temperatures is being studied. The "Gibbs free energy (G°), enthalpy (H°), and entropy (S°)" values for the adsorption of Fe (II) and Fe are shown in the table (III) (1) The sign carried a negative sign of G demonstrates the sustainability and impulsiveness. The procedure is endothermic, as indicated by the sign carried a positive of H, while this sign of S reveals the perfect affinity of the adsorbate to the adsorbent [37].



Fig. (20) : Relationship between ln Kd vs. 1/T for thermodynamic constants determination for Fe (II) onto a) CPH/ZnO  and b) CPH  , (pH=4, Co=50 mg/l, time=120min, particle size =125µm, and 150 rpm)
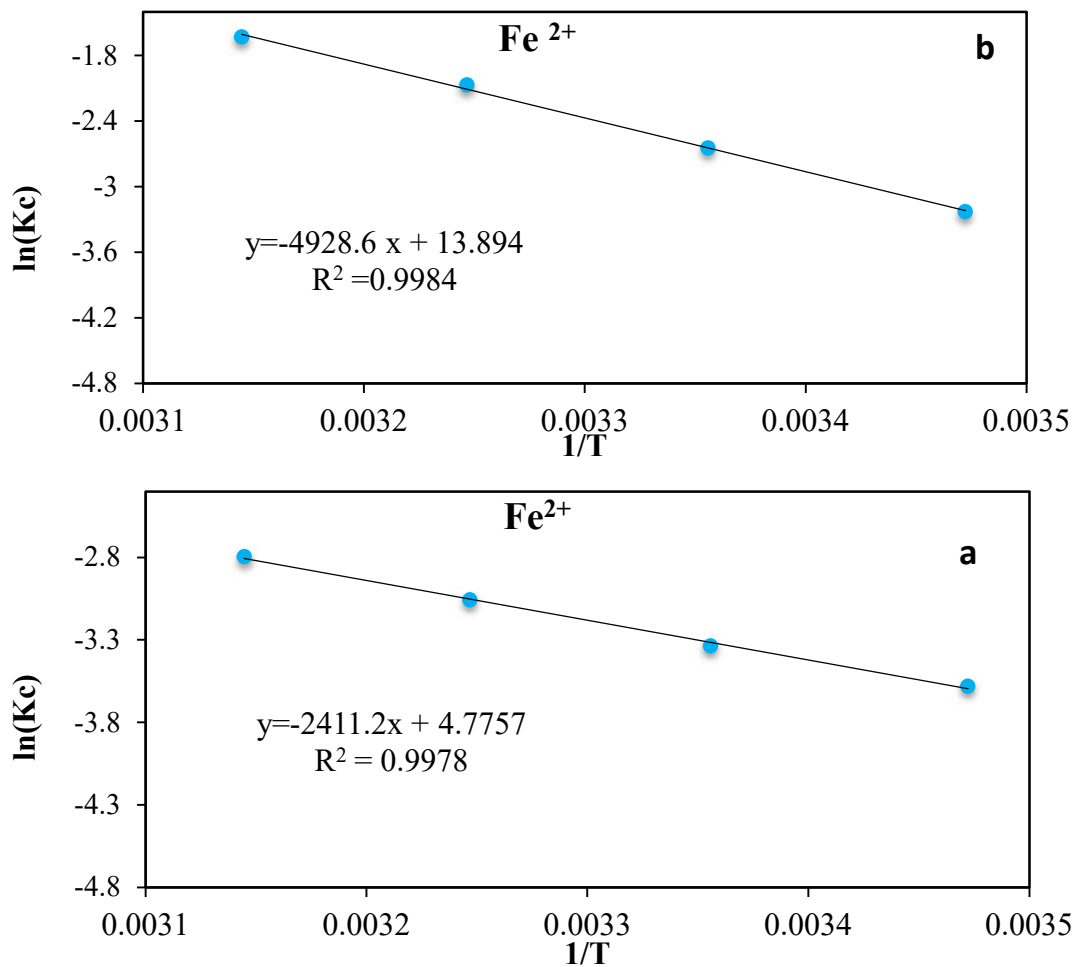
Fig. (21) : Relationship between ln Kd vs. 1/T for thermodynamic constants determination for Fe (III) onto a) CPH/ZnO  and b) CPH, (pH=4, Co=50 mg/l, time=120min, particle size =125μm, and 150 rpm)
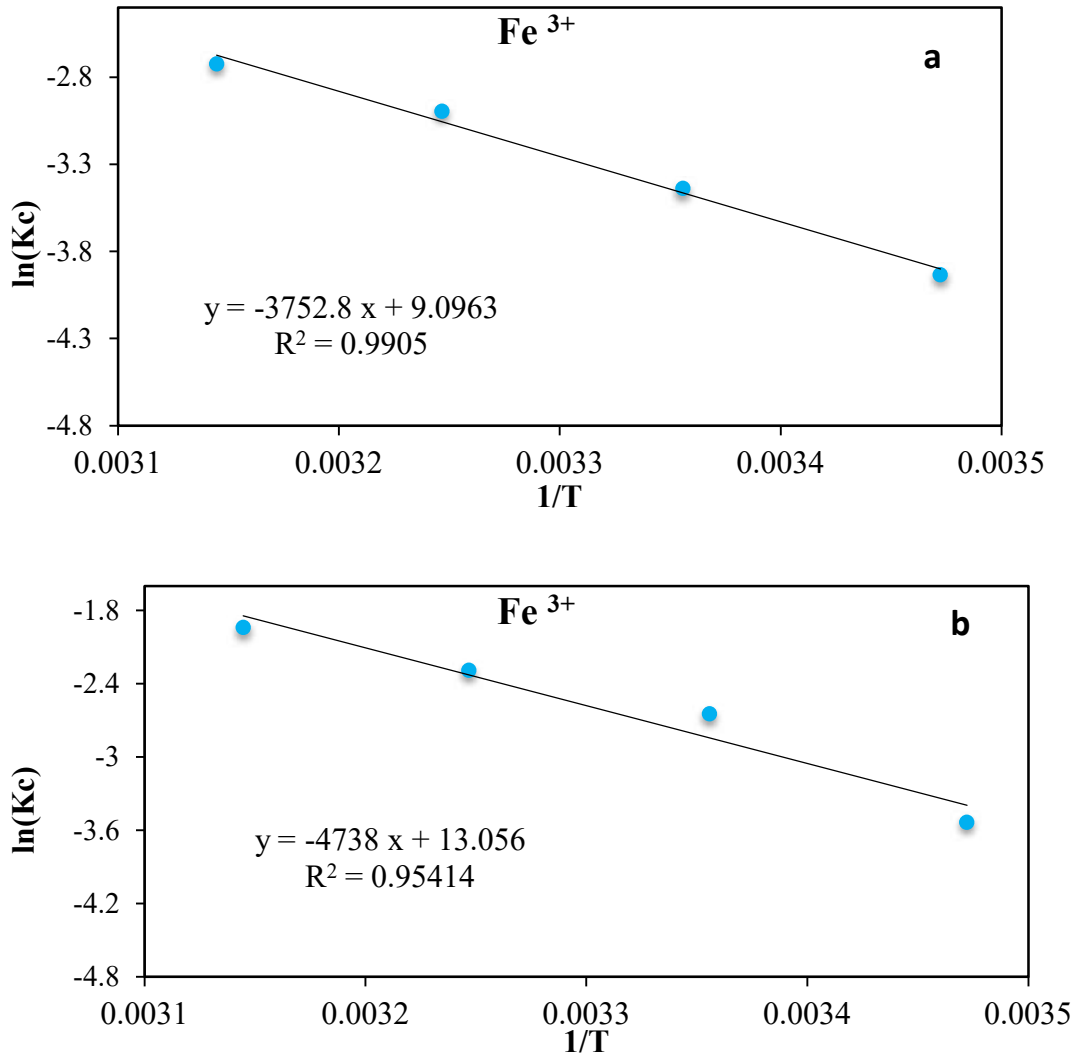
Table 1: "Thermodynamic parameters of Fe (II) and Fe (III) adsorption onto row and modified cowpea husk."

| metals | T (C°) | Cowpea husk | | | | ZnO- Cowpea husk | | | |
|---|---|---|---|---|---|---|---|---|---|
| | | $\Delta G°$ (kj/mol) | $\Delta H°$ (kj/mol) | $\Delta S°$ (j/mol K) | $R^2$ | $\Delta G°$ (kj/mol) | $\Delta H°$ (kj/mol) | $\Delta S°$ (j/mol K) | $R^2$ |
| Fe (II) | 15 | -0.0666 | 20.046 | 39.703 | 0.99 | -0.094 | 40.97 | 115.51 | 0.998 |
| | 25 | -0.088 | | | | -0.175 | | | |
| | 35 | -0.12 | | | | -0.323 | | | |
| | 45 | -0.16 | | | | -0.517 | | | |
| Fe (III) | 15 | -0.069 | 39.393 | 108.54 | 0.95 | -0.046 | 31.117 | 75.62 | 0.99 |
| | 25 | -0.175 | | | | -0.079 | | | |
| | 35 | -0.258 | | | | -0.128 | | | |
| | 45 | -0.38 | | | | -0.173 | | | |

## 4.4 isotherm study

Using two adsorption isotherms, namely the Langmuir and Freundlich models, it was explored how pollutants were absorbed on the surface of CPH and CPH/ZnO throughout the adsorption process. Adsorbent's isotherm of adsorption can be used to evaluate its capacity for adsorption and gain understanding of how both the surface-assimilative and the adsorbate retort. The model that best fits the equilibrium curve's correlation can offer insightful data regarding the adsorption mechanism [15]. Additionally, to provide a thorough grasp of the nature of interaction as depicted in figure (22) & (23). Table (2) displays the parameter values for the both models with the value of (R 2). The maximal metal uptake under the conditions presented is denoted by the parameter qmax, and the constant b is connected to the compatibility of the adsorbent with the adsorbate. The maximum capabilities for heavy metal adsorption onto row cowpea husk are 15.156 and 5.1432 mg/g for the two types of heavy metals. While the maximum capacities of chemically altered adsorbents are 6.183 and 4.487 mg/g for both two types of metals. Table 3 shows that the highest number of heavy metals onto row and modified cowpea husk is significantly higher when compared to earlier trials. The advantage of the adsorption technique depends on the value of RL (0<RL<1). The value of n (i.e., Freundlich intensity) (n>1) determines whether or not the adsorption is preferred. The more precise Langmuir Model is the one with the highest R2 value.
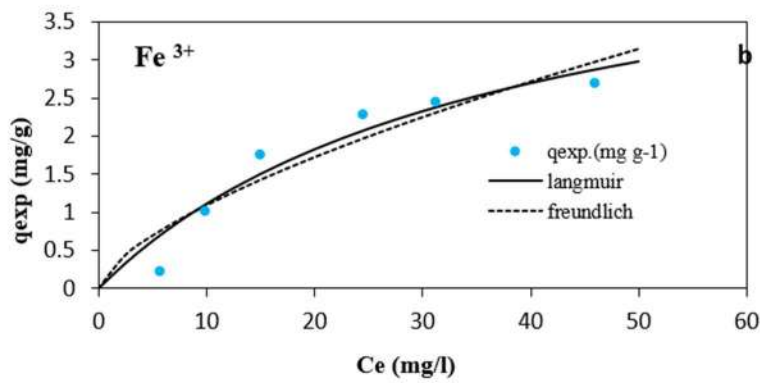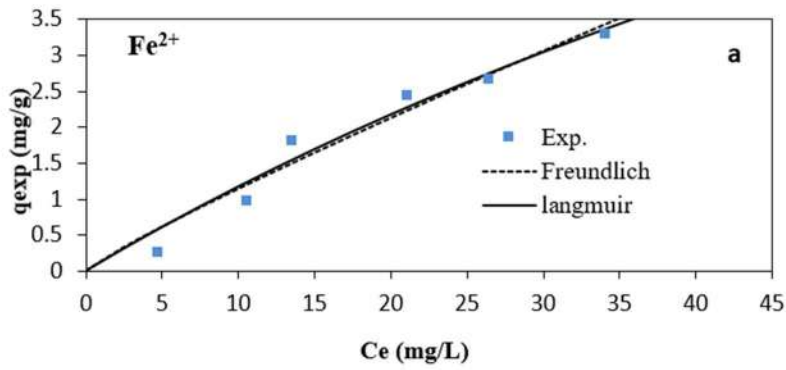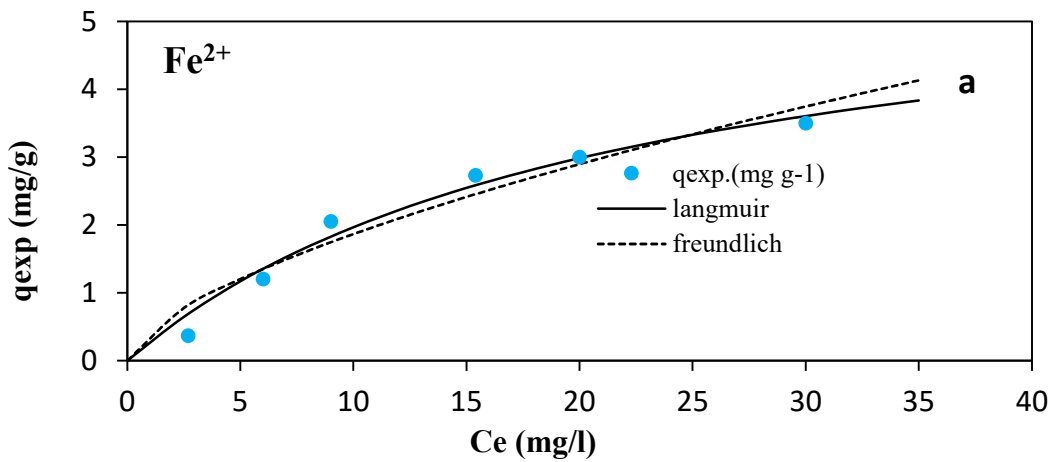
Fig. (22): "Sorption Isotherm of Langmuir and Freundlich model" for the a) Fe (II), and b) Fe (III) adsorption onto CPH".
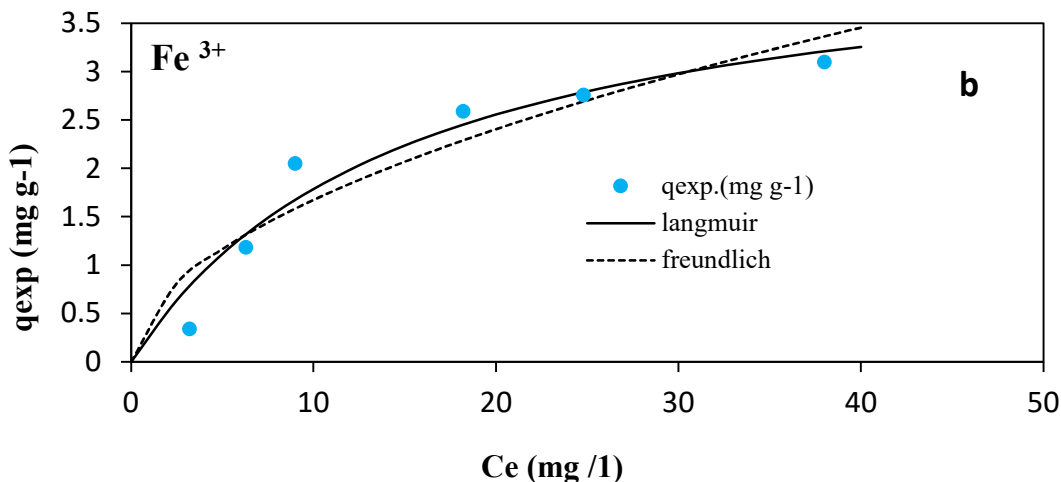
Fig. (23): "Sorption Isotherm of Langmuir and Freundlich" model for the a) Fe (II), and b) Fe (III) adsorption onto CPH/ZnO

Table 2: "Sorption Isotherm for Langmuir and Freundlich model" for the heavy metal's adsorption onto row and modified cowpea husk

| Model | parameters | Row Cowpea husk | | Coated Cowpea husk | |
|---|---|---|---|---|---|
| | | Fe (II) | Fe (III) | Fe (II) | Fe (III) |
| Freundlich Model | $K_f$ | 0.1445 | 0.242 | 0.433 | 0.5029 |
| | n | 1.114 | 1.524 | 1.576 | 1.0137 |
| | $R^2$ | 0.952 | 0.879 | 0.938 | 0.878 |
| Langmuir Model | $q_{max}$ | 15.156 | 5.143 | 6.183 | 4.487 |
| | b | 0.0087 | 0.027 | 0.046 | 0.066 |
| | $R^2$ | 0.959 | 0.923 | 0.972 | 0.935 |
| | $R_l$ | 0.7 | 0.445 | 0.3367 | 0.2726 |

Table 4.3: maximum adsorption capacity of Fe from previous studies

| Adsorbent | Adsorbate | qmax (mg/g) | REF. |
|---|---|---|---|
| Tannic acid immobilized AC | Fe (III) | 1.77 | [38] |
| rice husk | Fe (II) | 9.46 | [39] |

### 4.5 "Kinetic Study"

to give the reaction route and the ideal absorption mechanism valuable significance, the research of adsorption kinetics is important. In addition to the mass transfer process [15]. The effectiveness of adsorption, the technique by which the occurrence of adsorption happens, the time required to achieve balance and other consequences related to the adsorption rate are all crucially determined

by the kinetics study. An adsorbent must have a high adsorption rate if it is intended for use in wastewater treatment facilities [40]. Using some experimentations for the adsorption kinetics of the three metals onto adsorbents were inspected using "pseudo first order", "pseudo second order", and "intra-particle diffusion models" (26). Tables list the calculated parameter values that were obtained from applying these models in accordance with Eqs. (7–11). (4). Associating "$R^2$" for each applicable model and the congruence between the designed and investigational "qe" values allow for the identification of the most advantageous model. In Microsoft Excel 2019, nonlinear regression was used to calculate these kinetic model parameters. Higher R2 values and theoretical qe values that are close to experimental qe showed that the "second-order model is suitable for the adsorption behavior of all both two types of iron metals both row and modified adsorbent", as shown in the table (4). Additionally, the C values were greater than zero, showing that the rate-limiting adsorption process rather than intra-specific diffusion is responsible for the border layer's diffusion [41].
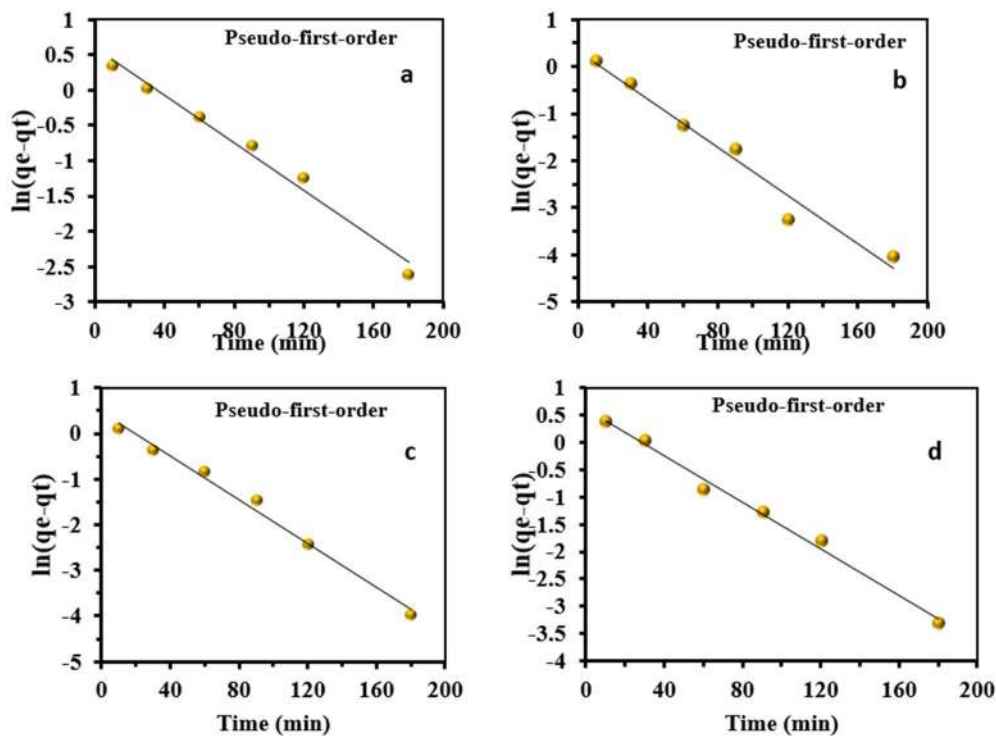


Fig. (24): "Pseudo-first-order" for (a, b) Fe (II) and (c, d) Fe (III) onto row and modified adsorbent correspondingly.
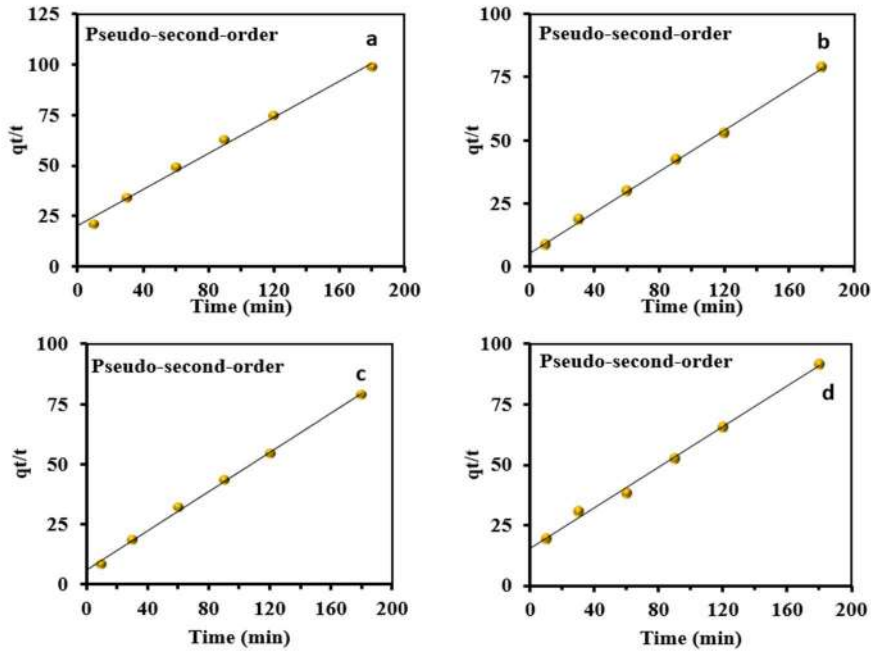
Fig. (25): Pseudo- second -order for (a, b) Fe (II) and (c, d) Fe (III) onto row and modified adsorbent correspondingly
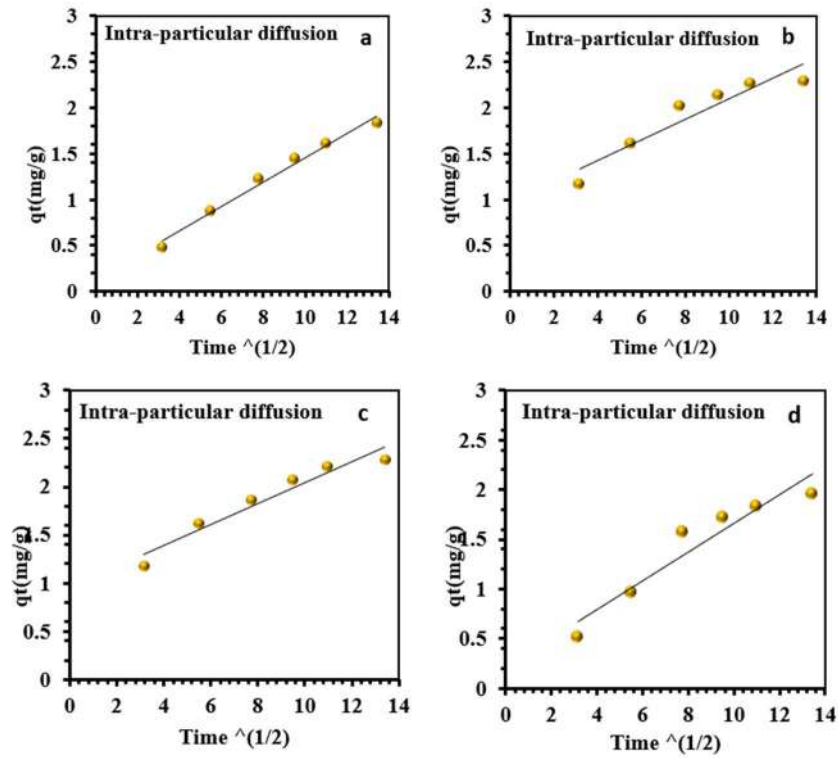
Fig. (26) : intraparticle- diffusion model for (a, b) Fe (II) and (c, d) Fe (III) onto row and modified adsorbent.

**Table 4: "Kinetic parameters of various models fitted for the sorption of heavy metals experimental data."**

| Model | parameters | Row Cowpea husk | | Coated Cowpea husk | |
|---|---|---|---|---|---|
| | | **Fe (II)** | **Fe (III)** | **Fe (II)** | **Fe (III)** |
| "Pseudo- first order" | $q_e$ | 1.855 | 1.806 | 1.65 | 1.892 |
| | $K_1$ | 0.017 | 0.025 | 0.027 | 0.021 |
| | $R^2$ | 0.986 | 0.986 | 0.97 | 0.993 |
| "Pseudo- second order" | $q_e$ | 2.231 | 2.455 | 2.46 | 2.388 |
| | $K_2$ | 0.01 | 0.027 | 0.03 | 0.0113 |
| | $R^2$ | 0.993 | 0.997 | 0.999 | 0.9955 |
| Intraparticle diffusion | C | 0.1328 | 0.956 | 0.9757 | 0.2172 |
| | $K_P$ | 0.1326 | 0.1089 | 0.1116 | 0.1449 |
| | $R^2$ | 0.983 | 0.9403 | 0.888 | 0.9136 |

## 5.    CONCLUSIONS

The ability of raw cowpea husk (CPH) and cowpea husk coated (CPHC) with nano zinc oxide (ZnO) to adsorbent and remove Fe2+ and Fe3+ is being examined in the present work. By using cutting-edge SEM, XRD, and FT-IR techniques, the raw cowpea husk (CPH) and cowpea husk coated (CPHC) with nano zinc oxide (ZnO) adsorbent were studied. The results confirmed that the produced adsorbent performed generally better with zinc oxide (ZnO) nanoparticles coated on the CPH than it did without the raw cowpea husk (CPH). This increased the adsorption capacity as well as the practical usage. "The isotherm analysis" were present on the surfaces of the raw cowpea husk (CPH) and the cowpea husk coated (CPHC) with nano-sized zinc oxide (ZnO) to react with $Fe^{2+}$ and $Fe^{3+}$. Conferring to the results of the "Langmuir model", for the $Cu^{2+}$ of raw cowpea husk (CPH) and cowpea husk coated (CPHC) with nanozinc oxide (ZnO) is as follows: the kinetic data for Fe2+ and Fe3+ can be accurately demonstrated by the "pseudo-second-order model". The analysis also showed that various processes were in charge of regulating the kinetic rate. According to the results of the current study, cowpea husk coated with nano-sized zinc oxide (ZnO) is a good adsorbent that may be employed in adsorption treatment systems to sequester $Fe^{2+}$ and $Fe^{3+}$.

## 6.    References:

[1]    M. Zaki, A. Maulana, F. Tirtayani, P. N. Alam, and H. Husin, "Nano-bentonite as a low-cost adsorbent for removal of mercury from aqueous solution," *J. Phys. Conf. Ser.*, vol. 1402, no. 5, 2019, doi: 10.1088/1742-6596/1402/5/055010.

[2]     M. J. M-Ridha, S. L. Zeki, S. J. Mohammed, K. M. Abed, and H. A. Hasan, "Heavy Metals Removal from Simulated Wastewater using Horizontal Subsurface Constructed Wetland," *J. Ecol. Eng.*, vol. 22, no. 8, pp. 243–250, 2021, doi: 10.12911/22998993/138869.

[3]     P. Sarin *et al.*, "Iron release from corroded iron pipes in drinking water distribution systems: Effect of dissolved oxygen," *Water Res.*, vol. 38, no. 5, pp. 1259–1269, 2004, doi: 10.1016/j.watres.2003.11.022.

[4]     B. Acemioğlu, "Removal of Fe(II) ions from aqueous solution by Calabrian pine bark wastes," *Bioresour. Technol.*, vol. 93, no. 1, pp. 99–102, 2004, doi: 10.1016/j.biortech.2003.10.010.

[5]     M. S. Salman, H. S. Alhares, Q. A. Ali, M. J. M-Ridha, S. J. Mohammed, and K. M. Abed, "Cladophora Algae Modified with CuO Nanoparticles for Tetracycline Removal from Aqueous Solutions," *Water, Air, Soil Pollut.*, vol. 233, no. 8, 2022, doi: 10.1007/s11270-022-05813-4.

[6]     J. Virkutyte and R. S. Varma, "Green synthesis of metal nanoparticles: Biodegradable polymers and enzymes in stabilization and surface functionalization," *Chem. Sci.*, vol. 2, no. 5, pp. 837–846, 2011, doi: 10.1039/c0sc00338g.

[7]     F. Wang, Y. Pan, P. Cai, T. Guo, and H. Xiao, "Single and binary adsorption of heavy metal ions from aqueous solutions using sugarcane cellulose-based adsorbent," *Bioresour. Technol.*, vol. 241, pp. 482–490, 2017, doi: 10.1016/j.biortech.2017.05.162.

[8]     M. T. Rahman, T. Kameda, S. Kumagai, and T. Yoshioka, "A novel method to delaminate nitrate-intercalated Mg–Al layered double hydroxides in water and application in heavy metals removal from waste water," *Chemosphere*, vol. 203, pp. 281–290, 2018, doi: 10.1016/j.chemosphere.2018.03.166.

[9]     T. Taher, R. Mohadi, D. Rohendi, and A. Lesbani, "Kinetic and thermodynamic adsorption studies of congo red on bentonite," *AIP Conf. Proc.*, vol. 1823, 2017, doi: 10.1063/1.4978101.

[10]     J. N. Chikwendu,  a C. Igbatim, and I. C. Obizoba, "Chemical Composition of Processed Cowpea Tender Leaves and Husks," *Int. J. Sci. Res. Publ.*, vol. 4, no. 5, pp. 1–5, 2014.

[11]     A. A. Mohammed, T. J. Al-Musawi, S. L. Kareem, M. Zarrabi, and A. M. Al-Ma'abreh, "Simultaneous adsorption of tetracycline, amoxicillin, and ciprofloxacin by pistachio shell powder coated with zinc oxide nanoparticles," *Arab. J. Chem.*, vol. 13, no. 3, pp. 4629–4643, 2020, doi: 10.1016/j.arabjc.2019.10.010.

[12]     M. A. Ibrahim *et al.*, "Simultaneous Adsorption of Ternary Antibiotics (Levofloxacin, Meropenem, and Tetracycline) by SunFlower Husk Coated with Copper Oxide Nanoparticles," *J. Ecol. Eng.*, vol. 23, no. 6, pp. 30–42, 2022, doi: 10.12911/22998993/147806.

[13]     A. M. Ayuba and B. Idoko, "Adsorption of Congo red dye from aqueous solution using raw cowpea ( Vigna Unguiculata ) husk," vol. 9, pp. 9–16, 2021.

[14]     S. J. Mohammed, M. J. M-Ridha, K. M. Abed, and A. A. M. Elgharbawy, "Removal of levofloxacin and ciprofloxacin from aqueous solutions and an economic evaluation using the electrocoagulation process," *Int. J. Environ. Anal. Chem.*, vol. 00, no. 00, pp. 1–19, Apr. 2021, doi: 10.1080/03067319.2021.1913733.

[15]     Mohammed, S. J. and Mohammed-Ridha, M. J., "Optimization of levofloxacin removal

from aqueous solution using electrocoagulation process by response surface methodology," *Iraqi J. Agric. Sci.*, vol. 52, no. 1, pp. 204–217, 2021, doi: 10.36103/ijas.v52i1.1252.

[16]    M. E. Ossman, M. Abdel Fatah, and N. A. Taha, "Fe(III) removal by activated carbon produced from Egyptian rice straw by chemical activation," *Desalin. Water Treat.*, vol. 52, no. 16–18, pp. 3159–3168, 2014, doi: 10.1080/19443994.2013.796895.

[17]    A. A. Mohammed, A. A. Najim, T. J. Al-Musawi, and A. I. Alwared, "Adsorptive performance of a mixture of three nonliving algae classes for nickel remediation in synthesized wastewater," *J. Environ. Heal. Sci. Eng.*, vol. 17, no. 2, pp. 529–538, 2019, doi: 10.1007/s40201-019-00367-w.

[18]    S. Beddiaf, S. Chihi, and Y. Leghrieb, "The determination of some crystallographic parameters of quartz, in the sand dunes of Ouargla, Algeria," *J. African Earth Sci.*, vol. 106, pp. 129–133, 2015, doi: 10.1016/j.jafrearsci.2015.03.014.

[19]    S. Boussaa, A. Kheloufi, N. B. Zaourar, and F. Kerkar, "Valorization of Algerian Sand for Photovoltaic Application.," *Acta Phys. Pol. A.*, vol. 130, no. 1, 2016.

[20]    A. A. H. Faisal, S. F. A. Al-Wakel, H. A. Assi, L. A. Naji, and M. Naushad, "Waterworks sludge-filter sand permeable reactive barrier for removal of toxic lead ions from contaminated groundwater," *J. Water Process Eng.*, vol. 33, p. 101112, 2020.

[21]    A. H. Ali, "Removal of Sulfamethoxazole, Sulfapyridine and Carbamazepine, from Simulated Wastewater Using Conventional and Nonconventional Adsorbents," *Int. J. Environ. Res.*, vol. 13, no. 3, pp. 487–497, 2019.

[22]    M. A. Renu, K. Singh, S. Upadhyaya, and R. K. Dohare, "Removal of heavy metals from wastewater using modified agricultural adsorbents," *Mater. Today Proc.*, vol. 4, no. 9, pp. 10534–10538, 2017, doi: 10.1016/j.matpr.2017.06.415.

[23]    Y. Wu *et al.*, "Functionalized agricultural biomass as a low-cost adsorbent: Utilization of rice straw incorporated with amine groups for the adsorption of Cr (VI) and Ni (II) from single and binary systems," *Biochem. Eng. J.*, vol. 105, pp. 27–35, 2016.

[24]    Y. S. Koay, I. S. Ahamad, M. M. Nourouzi, L. C. Abdullah, and T. S. Y. Choong, "Development of novel low-cost quaternized adsorbent from palm oil agriculture waste for reactive dye removal," *BioResources*, vol. 9, no. 1, pp. 66–85, 2014.

[25]    K. Shahul Hameed, P. Muthirulan, and M. Meenakshi Sundaram, "Adsorption of chromotrope dye onto activated carbons obtained from the seeds of various plants: Equilibrium and kinetics studies," *Arab. J. Chem.*, vol. 10, pp. S2225–S2233, 2017, doi: 10.1016/j.arabjc.2013.07.058.

[26]    T. A. H. Nguyen *et al.*, "Applicability of agricultural waste and by-products for adsorptive removal of heavy metals from wastewater," *Bioresour. Technol.*, vol. 148, pp. 574–585, 2013.

[27]    P. S. Kumar, S. Ramalingam, V. Sathyaselvabala, S. D. Kirupha, A. Murugesan, and S. Sivanesan, "Removal of cadmium (II) from aqueous solution by agricultural waste cashew nut shell," *Korean J. Chem. Eng.*, vol. 29, no. 6, pp. 756–768, 2012.

[28]    A. Gala and S. Sanak-Rydlewska, "A Comparison of Pb 2+ Sorption from Aqueous Solutions on Walnut Shells and Plum Stones.," *Polish J. Environ. Stud.*, vol. 20, no. 4, 2011.

[29]    S. L. Kareem and A. A. Mohammed, "Removal of Tetracycline from Wastewater Using Circulating Fluidized Bed," *Iraqi J. Chem. Pet. Eng.*, vol. 21, no. 3, pp. 29–37, 2020.

[30]    F. Qu and P. C. Morais, "The pH dependence of the surface charge density in oxide-based semiconductor nanoparticles immersed in aqueous solution," *IEEE Trans. Magn.*, vol. 37, no. 4, pp. 2654–2656, 2001.

[31]    Y. P. Ting, F. Lawson, and I. G. Prince, "Uptake of cadmium and zinc by the alga Chlorella vulgaris: Part 1. Individual ion species," *Biotechnol. Bioeng.*, vol. 34, no. 7, pp. 990–999, 1989.

[32]    A. Saeed, M. Iqbal, and M. W. Akhtar, "Removal and recovery of lead (II) from single and multimetal (Cd, Cu, Ni, Zn) solutions by crop milling waste (black gram husk)," *J. Hazard. Mater.*, vol. 117, no. 1, pp. 65–73, 2005.

[33]    Z. Lin, J. Li, Y. Luan, and W. Dai, "Application of algae for heavy metal adsorption: A 20-year meta-analysis," *Ecotoxicol. Environ. Saf.*, vol. 190, p. 110089, 2020.

[34]    L. Nouri, I. Ghodbane, O. Hamdaoui, and M. Chiha, "Batch sorption dynamics and equilibrium for the removal of cadmium ions from aqueous phase using wheat bran," *J. Hazard. Mater.*, vol. 149, no. 1, pp. 115–125, 2007.

[35]    M. Doğan and M. Alkan, "Adsorption kinetics of methyl violet onto perlite," *Chemosphere*, vol. 50, no. 4, pp. 517–528, 2003.

[36]    A. Gupta, S. Mahajan, and R. Sharma, "Evaluation of antimicrobial activity of Curcuma longa rhizome extract against Staphylococcus aureus," *Biotechnol. reports*, vol. 6, pp. 51–55, 2015.

[37]    S. Banerjee and M. C. Chattopadhyaya, "Adsorption characteristics for the removal of a toxic dye, tartrazine from aqueous solutions by a low cost agricultural by-product," *Arab. J. Chem.*, vol. 10, pp. S1629–S1638, 2017.

[38]    A. Üçer, A. Uyanik, and Ş. F. Aygün, "Adsorption of Cu (II), Cd (II), Zn (II), Mn (II) and Fe (III) ions by tannic acid immobilised activated carbon," *Sep. Purif. Technol.*, vol. 47, no. 3, pp. 113–118, 2006.

[39]    N. Hossain, S. Nizamuddin, and K. Shah, "Thermal-chemical modified rice husk-based porous adsorbents for Cu (II), Pb (II), Zn (II), Mn (II) and Fe (III) adsorption," *J. Water Process Eng.*, vol. 46, p. 102620, 2022.

[40]    A. M. Aljeboree, N. Radi, Z. Ahmed, and A. F. Alkaim, "The use of sawdust as by product adsorbent of organic pollutant from wastewater: adsorption of Maxilon blue dye.," *Int. J. Chem. Sci.*, vol. 12, no. 4, pp. 1239–1252, 2014.

[41]    S. Z. M. Gilani, "Adsorption Of Ciprofloxacin From WaterGilani, S. Z. M. (2018), 'Adsorption Of Ciprofloxacin From Water By Adsorbents Developed From Oat Hulls,' In the Department of Chemical and Biological Engineering University of Saskatchewan. By Adsorbents Developed Fr," *Dep. Chem. Biol. Eng. Univ. Saskatchewan*, no. April, 2018.